

Magnetic Properties of Some Molybdenum(V) Dimeric Coordination Compounds with Terminal Oxo-Ligands and Di- μ -oxo-, Di- μ -sulfido- or μ -Oxo- μ -sulfido- Bridges

Hanako KOBAYASHI,* Takashi SHIBAHARA,[†] and Norikiyo URYŪ^{††}

Faculty of Science and Technology, Keio University, Kohoku-ku, Yokohama 223

[†]Department of Chemistry, Okayama University of Science, Ridai-cho, Okayama 700

^{††}Department of Applied Science, Faculty of Engineering, Kyushu University, Higashi-ku, Fukuoka 812

(Received June 18, 1986)

Magnetic susceptibilities and electron spin resonances of Mo(V) dimers, $\text{Cs}_2[\text{Mo}_2\text{O}_2\text{S}_2(\text{ox})_2(\text{H}_2\text{O})_2] \cdot 2\text{H}_2\text{O}$, $\text{Ba}[\text{Mo}_2\text{O}_4(\text{ox})_2(\text{H}_2\text{O})_2] \cdot 3\text{H}_2\text{O}$, $(\text{pyH})_4[\text{Mo}_2\text{O}_2\text{S}_2(\text{NCS})_6]$, $(\text{pyH})_4[\text{Mo}_2\text{O}_4(\text{NCS})_6] \cdot \text{H}_2\text{O}$ and $(\text{pyH})_4[\text{Mo}_2\text{O}_3\text{S}(\text{NCS})_6]$ were observed at temperatures from 2 K to room temperature. The paramagnetic part of the magnetic susceptibilities of these compounds was small and approached zero with decreasing temperature. Under an applied magnetic field strength of 40 kOe, the susceptibilities had temperature independent regions but the spin susceptibilities derived from the electron spin resonances, observed at a magnetic flux density of about 3000 G, showed temperature dependences like antiferromagnetic dimers. This discrepancy was explained by a quasi alternating linear chain antiferromagnetic model. The corrections of the diamagnetic susceptibilities are discussed.

Molybdenum coordination compounds with sulfur containing ligands are found in many enzyme systems. The magnetic properties of such molybdenum coordination compounds are of interest because the mechanism of enzyme activity is strongly correlated with their magnetism. Within a limited moiety of molybdenum coordination compounds, that is, a Mo(V) dimeric ion with double bridges of oxygen or sulfur, there are many residual problems. A salt $[\text{C}_5\text{H}_5\text{MoO}_2]_2$,¹⁾ which has oxygen double bridges, is known to be diamagnetic from NMR observations. On the other hand, $\text{Na}_2[\text{Mo}_2\text{O}_4(\text{edta})] \cdot 4\text{H}_2\text{O}$ ²⁾ and $\text{Ba}[\text{Mo}_2\text{O}_2(\text{ox})_2] \cdot 5\text{H}_2\text{O}$,³⁾ both are oxygen double bridged, are reported to be paramagnetic. A salt sulfur-bridged $\text{Na}_2[\text{Mo}_2\text{O}_2\text{S}_2(\text{histidine})_2] \cdot \text{H}_2\text{O}$,⁴⁾ which seems to be similar to $\text{Na}_2[\text{Mo}_2\text{O}_4(\text{edta})] \cdot 4\text{H}_2\text{O}$ from the view point of magnetism, is diamagnetic and $\text{Ba}[\text{Mo}_2\text{O}_4(\text{C}_2\text{O}_4)_2] \cdot 5\text{H}_2\text{O}$ ⁵⁾ is considered to be diamagnetic. The molecular and crystal structures of paramagnetic $(\text{pyH})_4[\text{Mo}_2\text{O}_4(\text{NCS})_6] \cdot \text{H}_2\text{O}$ were analyzed by Jezowska-Trzebiatowska et al.⁶⁾ together with several related coordination compounds. She reported the molar magnetic susceptibilities of $(\text{pyH})_4[\text{Mo}_2\text{O}_4(\text{NCS})_6]$ in the range $(74\text{--}281) \times 10^{-6}$ CGSemu at room temperature.⁷⁾ The magnetic susceptibility of $(\text{pyH})_4[\text{Mo}_2\text{O}_4(\text{NCS})_6]$ reported by Mitchell and Williams,²⁾ is paramagnetic with a value of 157×10^{-6} (CGSemu) at 120 K and 147×10^{-6} (CGSemu) at 293 K. We have synthesized its homologous series $[\text{Mo}_2\text{O}_3\text{S}(\text{NCS})_6]$ and $[\text{Mo}_2\text{O}_2\text{S}_2(\text{NCS})_6]$ salts⁸⁾ and observed their magnetic susceptibilities and electron paramagnetic resonances, together with those of $[\text{Mo}_2\text{O}_4(\text{NCS})_6]$ salt.⁶⁾ The two dimeric salts $[\text{Mo}_2\text{O}_2\text{S}_2(\text{ox})_2(\text{H}_2\text{O})_2]$ and $[\text{Mo}_2\text{O}_4(\text{ox})_2(\text{H}_2\text{O})_2]$ also were prepared and measured to examine some common properties

among $\begin{array}{c} \text{O} & \text{S} & \text{O} \\ \parallel & \parallel & \parallel \\ \text{Mo} & \text{---} & \text{Mo} \\ \parallel & \parallel & \parallel \\ \text{O} & \text{S} & \text{O} \end{array}$, or $\begin{array}{c} \text{O} & \text{O} & \text{O} \\ \parallel & \parallel & \parallel \\ \text{Mo} & \text{---} & \text{Mo} \\ \parallel & \parallel & \parallel \\ \text{O} & \text{O} & \text{O} \end{array}$ skelton.

Experimental

Preparation of Samples. Caesium di- μ -sulfido-bis[aquaaxalatooxomolybdate(V)] dihydrate ($\text{Cs}_2[\text{Mo}_2\text{O}_2\text{S}_2(\text{ox})_2(\text{H}_2\text{O})_2] \cdot 2\text{H}_2\text{O}$ (1)) and barium di- μ -oxo-bis[aquaaxalatooxomolybdate(V)] trihydrate ($\text{Ba}[\text{Mo}_2\text{O}_4(\text{ox})_2(\text{H}_2\text{O})_2] \cdot 3\text{H}_2\text{O}$ (2)) were prepared following Refs. 5, 9, and 10. Pyridinium di- μ -sulfido-bis[tris(isothiocyanato)oxomolybdate(V)] ($(\text{pyH})_4[\text{Mo}_2\text{O}_2\text{S}_2(\text{NCS})_6]$ (3)) and pyridinium di- μ -oxo-bis[tris(isothiocyanato)oxomolybdate(V)] monohydrate ($(\text{pyH})_4[\text{Mo}_2\text{O}_4(\text{NCS})_6] \cdot \text{H}_2\text{O}$ (4)) were prepared by the method reported in Refs. 6, 7, and 11. Pyridinium μ -oxo- μ -sulfido-bis[tris(isothiocyanato)oxomolybdate(V)] ($(\text{pyH})_4[\text{Mo}_2\text{O}_3\text{S}(\text{NCS})_6]$ (5)) was prepared following the method in Ref. 8. Chemical analysis results were: Found: N, 14.64; C, 32.51; H, 2.36%. Calcd for 3: N, 14.64; C, 32.64; H, 2.53%. Found: N, 15.11; C, 33.26; H, 2.57%. Calcd for 4: N, 14.86; C, 33.12; H, 2.78%. Found: N, 14.87; C, 33.29; H, 2.50%. Calcd for 5: N, 14.89; C, 33.19; H, 2.57%.

Measurements of Magnetic Properties. Magnetic susceptibilities of samples 1, 2, 3, 4, and 5 were observed on powders in the temperature range from about 2 K to about 280 K by a magnetic balance (Oxford Instruments) of the Faraday method, which applies magnetic fields of a constant strength and a homogeneous gradient.^{12,13)} In order to prevent the powder sample from changing water content, it was put into a quartz cell together with minimum amount of liquid paraffin of special grade sufficient to cover the powder. The absolute values of the measured magnetic susceptibilities were small. Therefore, a constant magnetic field of 4×10^4 Oe and an inhomogeneous magnetic field with gradient of 390 Oe cm^{-1} were mainly used. The thermometer is fixed to the cryostat wall. The measurements of the $[\text{Cr}(\text{NH}_3)_6]\text{Cl}_3$ powder, which is paramagnetic in the temperature range from about 2 to 280 K, were made to correct the thermometer indications. For each measurement the sample cell site in the cryostat was checked, as were the pressures of the heat exchange gas and the time schedules of the temperature variation to get precise magnetic susceptibilities.

Electron spin resonances were observed on powder

samples and in CH_3CN solutions by a JEOL PE-3X with a microwave oscillator ES-SCXA. A thin-wall quartz cell was used. For CH_3CN solutions, signals were recorded with 1000 G/32 min scanning under 10 G modulation and input power of 0.8 mW. For powder samples measurements in the temperature range from about 2 K to 200–300 K were made using an Oxford Instruments' cryostat. Observations were made at 1000 G/40 min or 1000 G/16 min scanning rate under 1 or 10 G modulation with input power of 0.8 mW or 10^{-2} mW. The thermometer at the cryostat was calibrated by measurements of a $\text{Au}(\text{Co})$ -Cu thermocouple set at the sample position at a range of temperature variation made under the same conditions of changing rates and pressure of the atmosphere with the sample measurements. The magnetic flux densities were checked by diluted Mn^{10}O hyperfine interaction signals and the H_1 effect measurements were also checked by the diluted Mn^{10}O marker. The " H_1 effects" were observed in a range of input powers from 10^{-3} to 20 mW.

Units. The nonrationalized CGSemu are used in the present paper. The relations between the SI and the CGSemu systems on the units used in this paper are listed in Ref. 14.

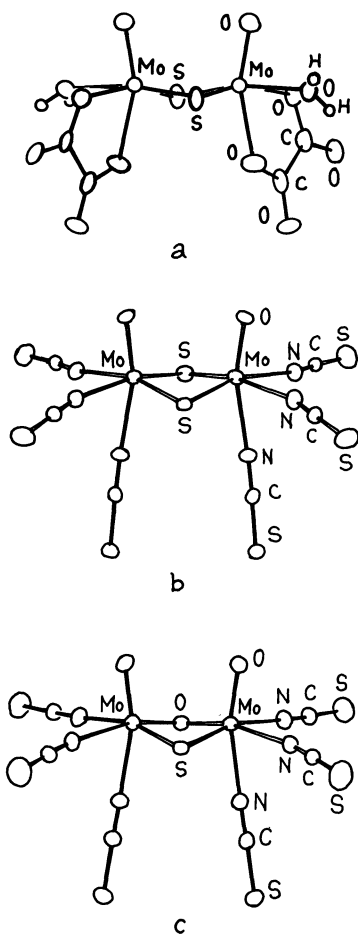


Fig. 1. Structures of complex ions from Ref. 8. (a): $[\text{Mo}_2\text{O}_2\text{S}_2(\text{ox})_2(\text{H}_2\text{O})_2]^{2-}$ ion, (b): $[\text{Mo}_2\text{O}_2\text{S}_2(\text{NCS})_6]^{4-}$ ion, (c): $[\text{Mo}_2\text{O}_3\text{S}(\text{NCS})_6]^{4-}$ ion.

Results and Discussion

Magnetic Susceptibility. The molybdenum complex ions of samples 1, 3, and 5 have the structures shown in Fig. 1. The structures of samples 2 and 4 are considered to be similar to 1 and 3, respectively.

The measured magnetic susceptibilities of samples 3, 4, and 5 were corrected for diamagnetism following Pascal's law. As no absorption was observed in the wavenumber region of the spectra below 10^4 cm^{-1} , no correction for the temperature independent paramagnetism was made. The molar magnetic susceptibilities of samples 3, 4, and 5 at room temperature obtained in this way were 1.7×10^{-4} , -0.27×10^{-4} , and $-4.4 \times 10^{-4} \text{ cm}^3$, respectively. However, the electron paramagnetic resonances observed on all the three samples in the temperature range from about 2 to 280 K showed that they were paramagnetic, and the results of chemical analyses and molecular structure analyses by X-ray diffraction,^{6,9)} also established that the three were dimers of Mo (V), which may have $S=1/2$ spin on each Mo ion. The values of the molar magnetic susceptibilities reported above show that they need more corrections for diamagnetic susceptibilities, namely, at least the corrections of anisotropic diamagnetic susceptibilities due to the looped structures, that is, the pyridinium ion and the

$\text{Mo} \text{---} \text{S} \text{---} \text{Mo}$, $\text{Mo} \text{---} \text{O} \text{---} \text{Mo}$ or $\text{Mo} \text{---} \text{S} \text{---} \text{Mo}$ structures. Lonsdale¹⁵⁾ showed that the aromatic rings gave rise to anisotropic diamagnetic susceptibilities. An aromatic π -bonding structure with an effective radius r has an anisotropic diamagnetic susceptibility of $\chi_{\text{ring}} = (-Ne^2/4mC^2) \sum_p r^2$, where N is the Avogadro number, p is the number of p -electrons in the π -bonding loop and other symbols have their usual meanings. The unit of χ_{ring} is CGSemu except e and r which are CGSesu and Å respectively. The projections of the area of π -bonding looped structures on the planes perpendicular to the external magnetic field directions of the samples were calculated in order to estimate the anisotropic diamagnetic susceptibilities. For the pyridinium ion, which is analogous to benzene, 6 electrons were taken as mobile electrons under the applied magnetic field. For the $\text{Mo} \text{---} \text{S} \text{---} \text{Mo}$ group, the following electronic

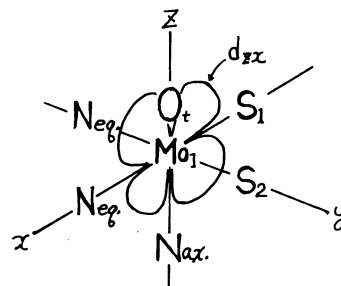


Fig. 2. Axes of atomic orbitals.

structure is assumed; a Mo^{5+} ion is basically six-coordinated with σ -bonding by two p-electrons from each bridged S^{2-} ion, two p-electrons from a terminal O^{2-} ion, two p-electrons from each equatorial N and two p-electrons from an axial N. If x, y, and z axes are taken as in Fig. 2, π -bondings are made up between d_{zx} of Mo_1 and p_z of S_1 , and d_{yz} of Mo_1 and p_z of S_2 , and, through the dimeric structure, a linked π -bonding is constructed. The π -bonding is a bound state like that in the aromatic benzene ring, but in this case the π -electrons might not be as mobile as those of the aromatic π -electrons. Thus, when the magnetic field is applied, four p_z -electrons of S-double bridges and two paramagnetic 4d electrons of two Mo^{5+} circulate along the π -bonding. The four p_z -electrons will contribute to the diamagnetism and two 4d electrons will effectively contribute to the paramagnetism; they have a spin of 1/2 respectively and would have super-exchange interactions of antiferromagnetic through the diamagnetic electrons as is predicted from the temperature dependence of the magnetic susceptibility derived from the ESR experiments as will be seen later. The electronic structure mentioned above is the simplest assumption for the Larmor rotation. The terminal O^{2-} would be coordinated to the Mo by four additional 2p-electrons, that is, between the Mo and the terminal O^{2-} , the bond order would therefore be higher than two. If so, the p orbitals might overlap with d_{zx} and d_{yz} of Mo. When the four 3p_z-electrons which originally belonged to the bridged S^{2-} ions rotate in the external magnetic field, eight 2p-electrons from two terminal O^{2-} ions and four p-type electrons from the equatorial two N atoms, where sp hybridization is considered, would also be brought into the π -bonding rotation. This is because the 2p_z orbitals of the equatorial two N atoms are overlapped with d_{yz} and d_{zx} respectively. If this extended π -bonding is assumed, a total of 16 electrons will rotate along the linkage. If sp hybridizations are assumed in the bridged S^{2-} , four additional electrons, making a total of 20 might contribute to the anisotropic dia-

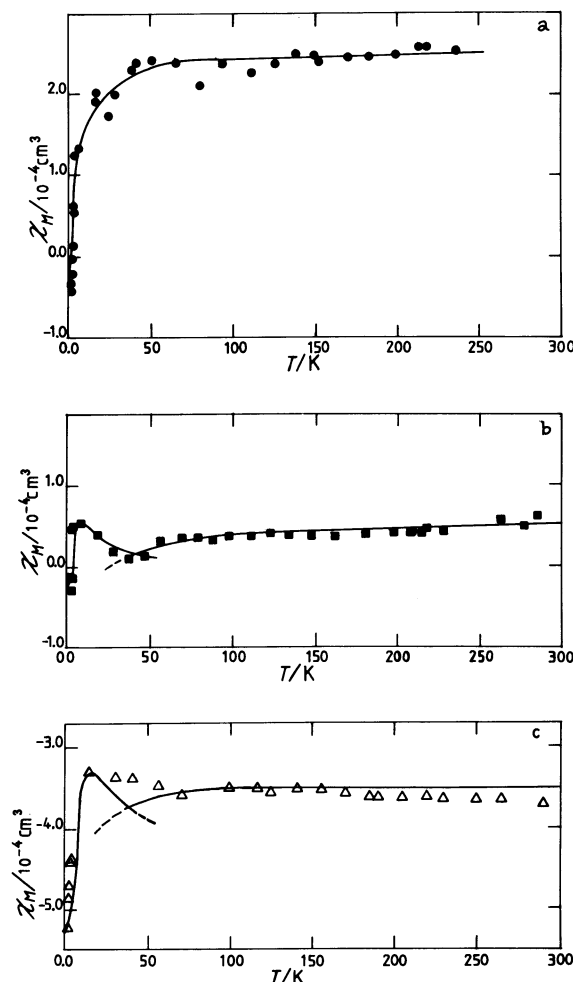


Fig. 3. Molar magnetic susceptibilities. (a): $(\text{pyH})_4[\text{Mo}_2\text{O}_2\text{S}_2(\text{NCS})_6]$ (3) (●: Experimental values. The diamagnetic susceptibility $-582 \times 10^{-6} \text{ cm}^3$ is corrected. The thin curve is a fitted $C_3 \exp(-5/T)$). (b): $(\text{pyH})_4[\text{Mo}_2\text{O}_4(\text{NCS})_6] \cdot \text{H}_2\text{O}$ (4) (■: Experimental values. The diamagnetic susceptibility $-527 \times 10^{-6} \text{ cm}^3$ is corrected. The thin curves are fitted $C_4 T^{-1/2} \exp(-14/T^2)$ and $C_4 \exp(-30/T)$). (c): $(\text{pyH})_4[\text{Mo}_2\text{O}_3\text{S}(\text{NCS})_6]$ (5) (△: Experimental values. The diamagnetic susceptibility $-577 \times 10^{-6} \text{ cm}^3$ is corrected. The thin curves are fitted $C_5 T^{-1/2} \exp(-60/T^2)$ and $C_5 \exp(-10/T)$).

Table 1. The Diamagnetic Susceptibilities^{a)} Used for the Correction of the Molar Magnetic Susceptibilities

	$\chi_{\text{atomic}}/(\text{CGSemu})^b)$	$\chi_{\text{ring}}/(\text{CGSemu})^c)$ cation	$\chi_{\text{ring}}/(\text{CGSemu})^d)$ anion
Sample (1)	-0.000268		-0.000004, -0.000014
Sample (2)	-0.000243		-0.000004, -0.000014
Sample (3)	-0.000502	-0.000072	-0.000008, -0.000034
Sample (4)	-0.000448	-0.000072	-0.000007, -0.000026
Sample (5)	-0.000498	-0.000072	-0.000007, -0.000030

a) The values are for one mol of the sample in CGSemu, then, their units are cm^3 . b) The magnetic susceptibility for mol due to the atomic diamagnetism. c) The magnetic susceptibility for mol due to four pyridinium ions. d) The magnetic susceptibility for mol due to a π -orbital containing two $\text{Mo}(\text{V})$'s. The former value is the case of 4 mobile p-electrons and the latter value is of 16 mobile p-electrons.

magnetism. For the $\begin{array}{c} \text{O} \quad \text{O} \\ \parallel \quad \parallel \\ \text{Mo} \cdots \text{O} \cdots \text{Mo} \\ \parallel \quad \parallel \\ \text{O} \quad \text{O} \end{array}$ and $\begin{array}{c} \text{O} \quad \text{O} \\ \parallel \quad \parallel \\ \text{Mo} \cdots \text{S} \cdots \text{Mo} \\ \parallel \quad \parallel \\ \text{O} \quad \text{O} \end{array}$ structures, the mobile electrons were similarly considered. The anisotropic diamagnetic molar susceptibilities are shown together with atomic diamagnetic susceptibilities in Table 1. The molar magnetic susceptibilities corrected for the diamagnetic susceptibilities are shown in Fig. 3.

The corrected value of sample 4 is in the same order value with that measured by Mitchell and Williams²⁾ for $(\text{pyH})_4[\text{Mo}_2\text{O}_4(\text{NCS})_6]$. Jezowska-Trzebiatowska et al.⁷⁾ measured more than five pyridinium salts of di- μ -oxo- and μ -oxo- μ -(sulfido, perchlorate, oxalato, or etc.)-bis[oxomolybdate(V)], the molar magnetic susceptibilities of which are in the same region with our data at room temperature. The temperature dependence of the molar magnetic susceptibilities of samples 3, 4, and 5 under the applied magnetic field of 40 kOe is roughly as follows. At very low temperature the molar magnetic susceptibilities increase exponentially with rising temperature from small values, reaching a maximum around 10–20 K, and retaining the same magnitude up to room temperature. This temperature dependence at very low temperatures

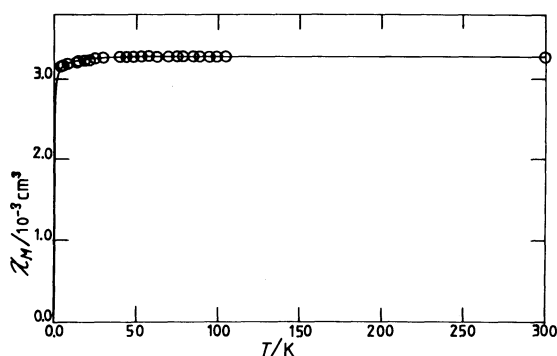


Fig. 4. The molar magnetic susceptibility of $\text{Cs}_2[\text{Mo}_2\text{O}_2\text{S}_2(\text{ox})_2(\text{H}_2\text{O})_2] \cdot 2\text{H}_2\text{O}$ (1). (○: Experimental values. The diamagnetic susceptibility $-272 \times 10^{-6} \text{ cm}^3$ is corrected. The thin curve is a fitted $C_1 \exp(-0.2/T)$).

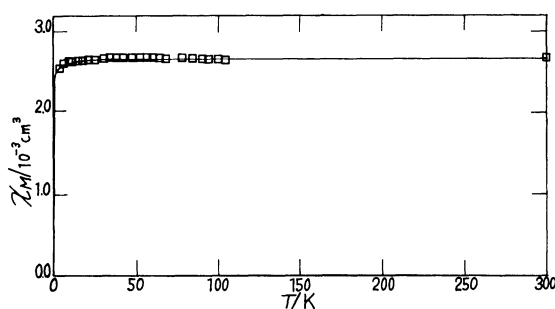


Fig. 5. The molar magnetic susceptibility of $\text{Ba}[\text{Mo}_2\text{O}_4(\text{ox})_2(\text{H}_2\text{O})_2] \cdot 3\text{H}_2\text{O}$ (2). (□: Experimental values. The diamagnetic susceptibility $-247 \times 10^{-6} \text{ cm}^3$ is corrected. The thin curve is a fitted $C_2 \exp(-0.2/T)$).

shows that it can be expressed in the form of $\exp(E/kT)$, where E is an activation energy and E/k would be about 10–20 K (k : Boltzmann's const. = $1.380662 \times 10^{-16} \text{ erg K}^{-1}$). The susceptibilities seem to decrease to zero at absolute zero K showing that the spins condense to a spin singlet state rather than to a long range ordered state. On the other hand from the temperature independent susceptibilities at higher temperatures we infer the existence of an ordered state. The isolated dimer spin system does not have any ordered state, and therefore an alternating linear chain system¹⁶⁾ or some other dimeric systems with

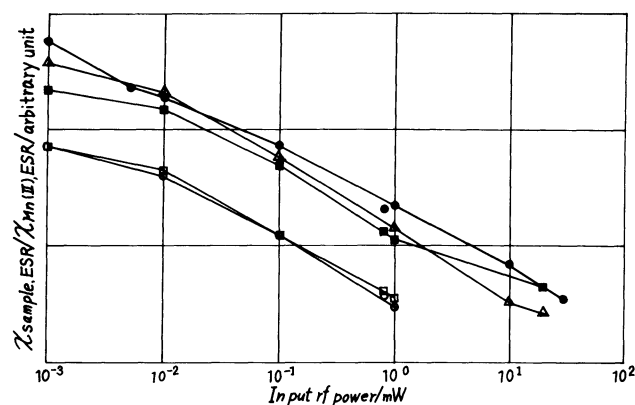


Fig. 6. The spin susceptibilities of the samples deduced from ESR's relative to that of diluted Mn^{2+} used as a reference versus input rf power. ○: $\text{Cs}_2[\text{Mo}_2\text{O}_2\text{S}_2(\text{ox})_2(\text{H}_2\text{O})_2] \cdot 2\text{H}_2\text{O}$ (1), □: $\text{Ba}[\text{Mo}_2\text{O}_4(\text{ox})_2(\text{H}_2\text{O})_2] \cdot 3\text{H}_2\text{O}$ (2), ●: $(\text{pyH})_4[\text{Mo}_2\text{O}_2\text{S}_2(\text{NCS})_6]$ (3), ■: $(\text{pyH})_4[\text{Mo}_2\text{O}_4(\text{NCS})_6] \cdot \text{H}_2\text{O}$ (4), △: $(\text{pyH})_4[\text{Mo}_2\text{O}_3\text{S}(\text{NCS})_6]$ (5).

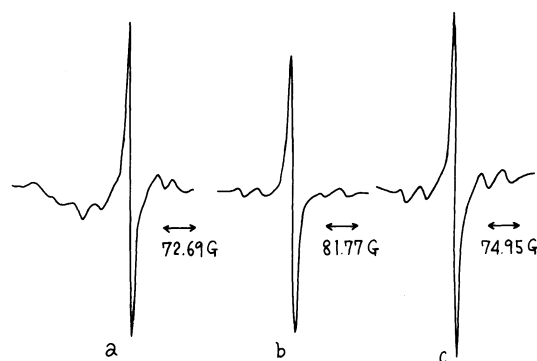


Fig. 7. ESR spectra. (a): $(\text{pyH})_4[\text{Mo}_2\text{O}_2\text{S}_2(\text{NCS})_6]$ (3) in CH_3CN solution at room temperature (Experimental conditions: 9.455 GHz, 0.8 mW, $3400 \pm 500 \text{ G}/64 \text{ min}$ scanning, and 10 G modulation. Results are listed in Table 2), (b): $(\text{pyH})_4[\text{Mo}_2\text{O}_4(\text{NCS})_6] \cdot \text{H}_2\text{O}$ (4) in CH_3CN solution at room temperature (Experimental conditions: 9.456 GHz, 0.8 mW, $3400 \pm 500 \text{ G}/32 \text{ min}$ scanning, and 10 G modulation. Results are listed in Table 2), (c): $(\text{pyH})_4[\text{Mo}_2\text{O}_3\text{S}(\text{NCS})_6]$ (5) in CH_3CN solution (Experimental conditions: 9.456 GHz, 0.8 mW, $3400 \pm 500 \text{ G}/64 \text{ min}$ scanning and 10 G modulation. Results are listed in Table 2).

interactions among the dimers should be present. As shown in Figs. 4 and 5, samples 1 and 2 showed similar and clearer temperature dependence of the magnetic susceptibilities with those of sample 3. The effective Bohr magneton numbers of the samples at 100 K were 1:1.6, 2:1.5, 3:0.45, and 4:0.21, respectively. Sample 5 was diamagnetic after the above diamagnetic corrections.

Electron Spin Resonance. The electron spin resonances were first observed to see if the samples are paramagnetic or not. All the samples showed paramagnetic resonances in the temperature region from 2 K to room temperature, in spite of the diamagnetic static susceptibility of sample 5. As mentioned in the section of the experimental the electron paramagnetic resonances were observed under unusual conditions. In Fig. 6, the magnetic susceptibilities derived from the ESR signals at room temperature divided by the magnetic susceptibilities of the diluted Mn^{2+} compounds used as a reference of the ESR signals were plotted for the ESR input

powers. All the samples showed decreasing intensities with increasing input powers, namely, a saturation effect called the " H_1 effect" was observed. Input power of 10^{-3} mW does not give the maximum signal intensity. This H_1 effect might be the reason why they reported that no ESR was observed in some Mo(V) dimeric coordination compounds.⁶⁾ The values of H_1 were not measured, but as at the same input power the diluted Mn^{2+} compound did not show any saturation. We believe that the input power of 0.8 mW was less than several G^2 as H_1^2 . Which of T_1 , T_2 , or, both of T_1 and T_2 are responsible for the ESR signal saturations cannot be decided, but this effect is never found in the reports of ESR of Mo(V) monomer, then, the " H_1 effect" would arise from the dimeric structures of the samples. The distances between the Mo(V) ions in the dimers are about 2.5–2.8 Å, but the effective superexchange interactions between the paired Mo(V) ions might be small, making T_2 long, alternatively spins in the π -molecular orbitals might have a large relaxation time to the lattice of the bath.

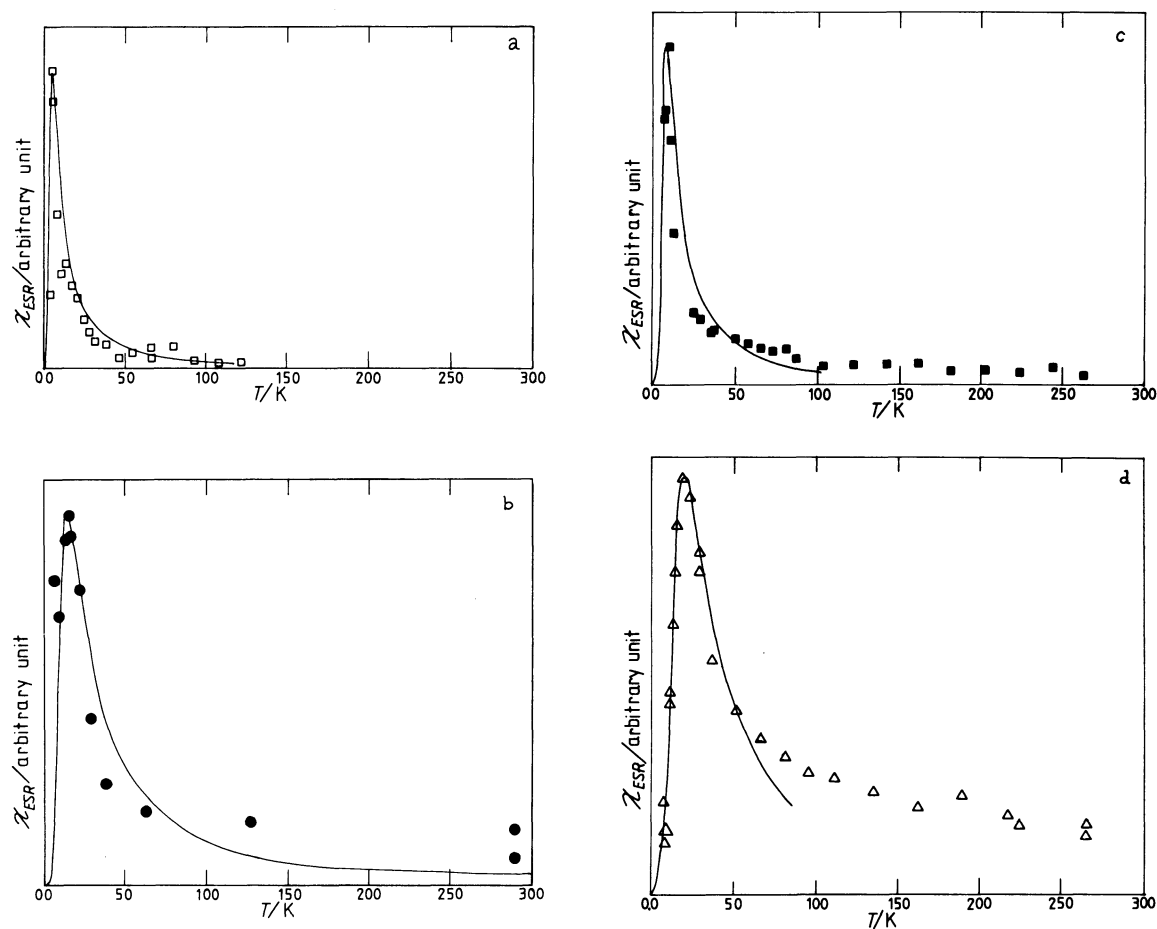


Fig. 8. Spin susceptibilities deduced from the ESR derivative curves versus temperatures. (a): $\text{Ba}[\text{Mo}_2\text{O}_4(\text{ox})_2(\text{H}_2\text{O})_2] \cdot 3\text{H}_2\text{O}$ (2) (\square : Experimental values and the thin curve is a fitted $B_2 T^{-3/2} \exp(-20/T^2)$). (b): $(\text{pyH})_4[\text{Mo}_2\text{O}_2\text{S}_2(\text{NCS})_6]$ (3) (\bullet : Experimental values and the thin curve is a fitted $B_3 T^{-3/2} \exp(-160/T^2)$). (c): $(\text{pyH})_4[\text{Mo}_2\text{O}_4(\text{NCS})_6] \cdot \text{H}_2\text{O}$ (4) (\blacksquare : Experimental values and the thin curve is a fitted $B_4 T^{-3/2} \exp(-40/T^2)$). (d): $(\text{pyH})_4[\text{Mo}_2\text{O}_3\text{S}(\text{NCS})_6]$ (5) (\triangle : Experimental values and the thin curve is a fitted $B_5 T^{-3/2} \exp(-260/T^2)$).

In Fig. 7, ESR derivative curves of samples 3, 4, and 5 in CH₃CN solutions at room temperature are shown, of which averaged g -values, H_{msl} 's (separation of maximum slope) and the hyperfine interaction splittings observed at 0.8 mW input power are listed in Table 2. The hyperfine interaction splittings were observed also on powder samples as listed in Table 3 together with g -values and H_{msl} 's. The ESR signals of samples 3, 4, and 5 showed isotropic g -values. Samples 1 and 2 showed g -values of axial anisotropy. Relative intensities of g_1, g_2 , and g_3 signals of sample 2 showed temperature dependences.

In Fig. 8, the spin susceptibilities obtained from the ESR signals by integration of the derivative curves of samples, 2, 3, 4, and 5 respectively are shown in arbitrary units in the temperature region from 2 K to

room temperature. The values at low temperatures seem to decrease to zero with decreasing temperatures. The spin susceptibilities have maxima at rather low temperatures; at higher temperatures they decrease with increasing temperature. This behavior is that of dimer spins or alternating linear spins¹⁶ or ladder model spins,¹⁶ though the peaks of the maxima are too steep to fit the theoretical dimer or alternating linear chain models. The different temperature dependences of a static magnetic susceptibility and a dynamic magnetic susceptibility are known as characteristic of the itinerant ferromagnetism in the theory on the weak ferromagnetic metals.¹⁷ This is an attractive theory having various suggestive ideas. However in our samples, the itinerant interactions are limited within the π -molecular orbitals, therefore it

Table 2. ESR Results of CH₃CN Solutions and Powder Samples at Room Temperature

	CH ₃ CN solution			Powder		
	g_{av} -value	Hyperfine splitting/G	H_{msl} /G	g_{av} -value	Hyperfine splitting/G	H_{msl} /G
Sample (1)				1.995		4.53
Sample (2)				1.996		4.19
Sample (3)	1.933	48.95	13.6	1.933	50.24	14.4
Sample (4)	1.934	49.29	15.0	1.935	39.80	24.5
Sample (5)	1.931	49.06	13.6	1.935	36.76	18.7

Table 3. Crystal Structure Parameters

	Space group Z	Lattice constants /Å /degree	Mo-Mo distance in a dimer /Å	Effective area of π -orbital linked two Mo's /(Å) ²	Effective area of π -orbital of pyridinium ion /(Å) ²	Mo-Mo distance of the nearest in the nearest neighbour /Å
Sample (1)	$P2_1/c$ 4	$a=12.427$ $b=16.197$ $c=9.590$ $\beta=109.77$	2.52—2.54	1.99		4.07—6.63
Sample (2)	$P3_121$ 6	$a=10.630$ $b=10.630$ $c=11.65$ $\gamma=120$	2.54	1.99		5.64
Sample (3)	$P2_1/m$ 2	$a=15.669$ $b=13.106$ $c=9.173$ $\beta=96.77$	2.83	4.77	6.70	15.0
Sample (4)	$Pna2_1$ 4	$a=26.161$ $b=15.106$ $c=9.755$	2.58 ^{a)}	3.59	6.70	
Sample (5)	$P2_1/m$ 2	$a=15.898$ $b=13.207$ $c=9.085$ $\beta=94.04$	2.69	4.17	6.70	13.5

a) Ref. 6.

should not be considered in the present case.

Alternating Linear Chain Magnet Model. The arrangements of the molecules in the crystals of the five dimer samples were investigated.^{5,8} Their space groups, lattice constants, numbers of Mo in a unit cell, distances between two Mo's of intra dimer and between a Mo and the nearest Mo in the nearest neighbour dimer, effective areas of the π -orbitals containing two Mo's and the π -orbital of pyridinium ion are listed in Table 3. In sample 1,⁸ the dimer complex ions make linear chains along the c axis, but it is not distinctly so, rather it should be said the dimer complex ions make two dimensional arrangements on the bc planes. Sample 2 has a spiral structure along the c axis where the molecular axes of the three dimer complex ions in a unit cell point in different directions consistent with the complex g -values observed in the ESR. Samples 3 and 5 have linear chains of the dimer complex ions along the b axis respectively. The details of sample 4 are not yet clear, but the five dimer samples are considered as magnetically alternating linear chains or dimers having low dimensional magnetic interactions among them.

The magnetic ordered state induced by the applied magnetic field was experimentally found on an alternating linear chain compound $\text{Cu}(\text{NO}_3)_2 \cdot 2.5\text{H}_2\text{O}$ by Amaya et al. and discussed by Tachiki et al., Bonner et al., and others.¹⁶ In Fig. 9, a phase diagram of the alternating linear chain of Heisenberg spins proposed by Bonner is shown. She considers that the ordered SF (spin flop) phase has a temperature independent magnetic susceptibility and at lower applied magnetic fields than the SF phase region the spins behave as an alternating linear chain. She reported the results of the exact calculations of the magnetic and thermal properties of the alternating linear chain of a finite number of spins up to 10 and

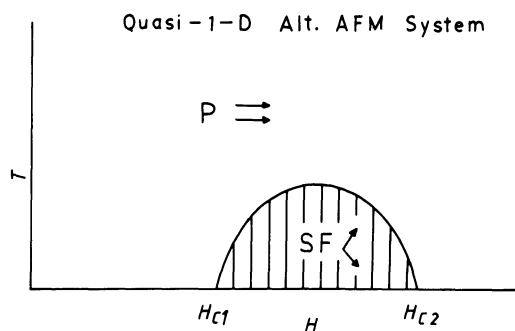


Fig. 9. A phase diagram of the quasi-1D alternating antiferromagnetic Heisenberg spins from Ref. 16. $P \rightleftharpoons$ shows paramagnetic phase under applied magnetic field, $SF \rightleftharpoons$ shows spin flopped phase of magnetic ordered phase induced by applied magnetic field; H_{c1} and H_{c2} are the critical magnetic fields at zero temperature.

extended them to the infinite number of spins. On the other hand, she gave a rough temperature dependence of the magnetic susceptibility of the alternating linear chain under applied magnetic fields lower than the critical SF phase field as $\chi = T^{-1/2} \exp(-\Delta E_1/kT)$. This is a good approximation at low temperatures. As described above, samples 1, 2, 3, and 4 measured at 40 kOe of an applied magnetic field and sample 5 measured at 10 kOe of an applied field showed temperature independent magnetic susceptibilities at higher temperatures than some temperatures characteristic to each sample. If the molar magnetic susceptibilities at temperatures above the constant values under the applied magnetic fields are expressed as C_i , where the base line is set at the value of zero K, the molar magnetic susceptibilities of the samples 1, 2, 3, 4, and 5 under the magnetic fields are $C_1 \exp(-0.2/T)$, $C_2 \exp(-0.2/T)$, $C_3 \exp(-5/T)$, $C_4 \exp(-30/T)$, and $C_5 \exp(-10/T)$, respectively, which are shown in Figs. 4, 5, and 3 a, b, and c. It can be assumed that the samples take ordered states under high applied magnetic fields having the magnetic susceptibilities of the C_i 's. If the spins are localized at atomic sites the magnetic susceptibilities will take the values of the ordered states as soon as the magnetic fields are applied at a low temperature. However the Mo(V) spins in the present samples are in the π -bonding linked orbitals. When the magnetic field is applied for the measurements at a low temperature, the mobile electrons and electron spins will begin the Larmor rotations. The rotations of the spins will attenuate with rising temperature to some velocities characteristic to each linked orbital and the spins will gradually take the ordered state values following the temperature dependences as shown in the graphs. The rotations of the nonmagnetic electrons will not have this temperature dependence. The electron spin resonances were observed at the magnetic flux densities of about 3000 ± 15 G. The observed temperature dependences of the spin susceptibilities derived from the ESR signals show that 3000 ± 15 G is lower than the critical fields of the SF ordered states, but the Larmor rotation will similarly affect the mobile electrons when the magnetic field is applied. At least the temperature dependence of the alternating linear chain magnetic susceptibilities of the five samples might have a term $\exp(-\Delta E'/T^2)$ instead of the Bonner's term $\exp(-\Delta E_1/T)$. The fitted magnetic susceptibilities to the experimental values of samples 2, 3, 4, and 5 were $B_2 T^{-3/2} \exp(-20/T^2)$, $B_3 T^{-3/2} \exp(-160/T^2)$, $B_4 T^{-3/2} \exp(-40/T^2)$, and $B_5 T^{-3/2} \exp(-260/T^2)$, respectively, where B_i 's are arbitrary constants. These fitted curves are drawn in Fig. 8 a, b, c, and d. The term $T^{-1/2}$ multiplied to the Bonner's term $T^{-1/2}$ might come from the rf field. We cannot decide whether this temperature dependence comes from an isothermal effect or from some relaxation effect due to

the method of ESR measurements. The curves of the fitted magnetic susceptibilities agree with the experimental curves at low temperatures, but at temperatures higher than the susceptibility maximum, the fittings become poorer with rising temperature as the curves never approach the Curie-Weiss type temperature dependence. The static magnetic susceptibility of sample 4 shows a different behavior. Its Larmor rotation effect is $C_4 \exp(-30/T)$ as mentioned above. Then before the spins reach the ordered state value the behavior as an alternating linear chain with the rotation effect appears with a fitted formula $C_{41} T^{-1/2} \exp(-14/T^2)$, as shown in Fig. 3. Sample 5 showed negative susceptibility after the above-mentioned atomic (Pascal) and molecular (π -orbital) orbital diamagnetism corrections have been applied. This sample was measured at an applied field of 40 kOe in the lower temperature region and at 10 kOe above 100 K. In the lower temperature region an alternating linear chain type susceptibility fitted to $C_{51} T^{-1/2} \exp(-60/T^2)$ is observed. For the superexchange interaction parameter J between two paramagnetic ions of spin 1/2 with double bridges each through one anion path are known to show a larger value than one hundred K, if it is expressed as $|J|/k$. For the present samples, if the exponential term of the spin susceptibilities derived from ESR signals indicates the band gap energy, then the superexchange interaction parameters of samples 2, 3, 4, and 5 are $|-100|$, $|-32|$, $|-1.3|$, and $|-26|$ K, respectively, where the rotation effects are removed. These values are small, though they are not inconsistent with the " H_1 effect".

The problem remains that sample 5 is diamagnetic after all the above-mentioned diamagnetic corrections have been applied. There may be some diamagnetism with large absolute values, not only in the sample 5 but in all the samples. The atomic diamagnetic susceptibility is $\chi = (-Ne^2/6mc^2) (\sum r_i^2)$, which was deduced from Larmor's theorem by Langevin and Pauli,¹⁸⁾ that is, the Larmor's rotation in the atomic core is considered as the ideal one, where electrons rotate along an orbital on a plane energy level. This assumption is used in the case of benzene π -orbital by Lonsdale. The static magnetic susceptibility is $\chi = M/H$, where M is magnetization and H is magnetic field strength, when the magnetic induction B is defined as $B = \mu H = H + 4\pi M$, $\chi = (\mu - 1)/4\pi$. When the sample is a superconductor, B is zero, that is, permeability μ should be zero. We consider, here, for normal substances, therefore, $0 < \mu$. On the other hand, we consider diamagnetism, therefore, χ should be negative, that is $\mu < 1$. When the electrons obey the ideal Larmor's theorem, $\chi \doteq -10^{-6} \text{ cm}^3$, that is $1 - \mu = +10^{-6} \times 4\pi$, namely, B/H is very near to 1. In the present samples, when a magnetic field is applied, mobile electrons circulate along molecular orbitals which are $\begin{array}{c} \text{O} & \text{O} \\ \parallel & \parallel \\ \text{---Mo---S---Mo---} \\ \parallel & \parallel \\ \text{O} & \text{O} \end{array}$, or $\begin{array}{c} \text{O} & \text{O} & \text{O} \\ \parallel & \parallel & \parallel \\ \text{---Mo---O---Mo---} \\ \parallel & \parallel & \parallel \\ \text{O} & \text{O} & \text{O} \end{array}$, or $\begin{array}{c} \text{O} & \text{O} & \text{O} \\ \parallel & \parallel & \parallel \\ \text{---Mo---S---Mo---} \\ \parallel & \parallel & \parallel \\ \text{O} & \text{O} & \text{O} \end{array}$. In

the above-mentioned corrections we have assumed ideal Larmor rotations, but, the results show us that the assumptions used were not suitable. B/H may be much smaller than 1 and the samples may have diamagnetic susceptibilities with large absolute values. If so the symmetry of the molecular orbital of sample 5 is lower than those of samples 3 and 4, and has diamagnetic susceptibility with the largest absolute value. This is consistent with the above considerations. Another possibility for the diamagnetism with a large absolute value, was proposed by Ginzburg¹⁹⁾ concerning the diamagnetism of CuCl and CdS. The diamagnetism would be due to the toroidal moment. He did not discuss coordination compounds, but if ring structures with mobile electrons take a toroidal coil arrangement in a crystal, the toroidal moment will appear. That possibility cannot be denied in samples 3, 4, and 5.

The authors wish to express their sincere thanks to Professor Minoru Kinoshita and Dr. Tadashi Sugano, the University of Tokyo, for the valuable discussions all over this work. The authors wish to express their thanks to the Institute for Molecular Science, Okazaki, and the Institute for Solid State Physics, the University of Tokyo, for the measurements of the magnetic susceptibilities and Professor Tadamasa Shida, Kyoto University, for the observations of the electron spin resonances. One of the authors (H. K.) would like to thank Professor Ikuji Tsujikawa, Dr. Yoshitami Ajiro, and Dr. Kiminori Ushida, Kyoto University, for the valuable discussions and Dr. Keisaku Kimura and Mr. Shunji Bandow, Institute for Molecular Science, for their thoughtful advice and helps with the measurements.

References

- 1) M. Cousins and M. L. H. Green, *J. Chem. Soc.*, **1964**, 1567.
- 2) P. C. H. Mitchell and R. J. P. Williams, *J. Chem. Soc.*, **1962**, 4570.
- 3) C. M. French and J. H. Garside, *J. Chem. Soc.*, **1962**, 2006.
- 4) B. Spivak and Z. Dori, *J. Chem. Soc., D*, **1970**, 1716.
- 5) F. A. Cotton and Sheila M. Morehouse, *Inorg. Chem.*, **4**, 1377 (1965).
- 6) B. Jezowska-Trzebiatowska, T. Glowiak, M. F. Rudolf, M. Sabat, and J. Sabat, *Russ. J. Inorg. Chem.*, **22**, 1590 (1977).
- 7) B. Jezowska-Trzebiatowska, M. F. Rudolf, L. Natkaniec, and H. Sabat, *Inorg. Chem.*, **13**, 617 (1974).
- 8) T. Shibahara, H. Kuroya, K. Matsumoto, and S. Ooi, *Bull. Chem. Soc. Jpn.*, **56**, 2945 (1983), W. S. McDonald, *Acta Crystallogr., Sect. B*, **34**, 2850 (1978).
- 9) F. A. Armstrong, T. Shibahara, and A. G. Sykes, *Inorg. Chem.*, **17**, 189 (1978).
- 10) R. G. James and W. Wardlaw, *J. Chem. Soc.*, **1927**, 2152.

- 11) N. H. Furman and C. O. Miller, *Inorg. Synth.* **3**, 160 (1950).
 12) M. Takahashi, T. Sugano, and M. Kinoshita, *Bull. Chem. Soc. Jpn.*, **57**, 26 (1984).
 13) K. Kimura and S. Bandow, *Kotai Butsuri*, **19**, 31 (1984).
 14) List of units and conversions

	SI unit system	CGSemu non- rationalized system of unit
B : Magnetic flux density	T=Wbm ⁻²	G
H : Strength of magnetic field	Am ⁻¹	Oe
M : Magnetization	Am ⁻¹	
χ_M : Molar magnetic susceptibility	m ³	cm ³
<hr/>		
3.336 × 10 ⁻¹⁰ /coulombs = 1/e.s.u. of elec. charge		
10 ⁻⁴ /T = 1/G		
10 ³ × 4π/Am ⁻¹ = 1/Oe		
(χ _M in SI)/m ³ = 4π × 10 ⁻⁶ (χ _M in CGSemu)/cm ³		

- 15) K. Lonsdale, *Proc. R. Soc. London, Ser. A.* **159**, 149 (1936).
 16) J. C. Bonner, S. A. Friedberg, H. Kobayashi, D. L. Meier, and H. W. J. Blote, *Phys. Rev. B* **27**, 248 (1983).
 17) T. Moriya and A. Kawabata, *J. Phys. Soc. Jpn.*, **34** 639 (1973), *ibid.* **35**, 669 (1973); H. Hasegawa and T. Moriya, *J. Phys. Soc. Japan*, **36**, 1542 (1974); T. Moriya, *J. Magn. Magn. Mag.* **14**, 1 (1979); H. Capellmann, *Z. Physik, B* **34**, 29 (1979).
 18) J. H. Van Vleck, "The Theory of Electric and Magnetic Susceptibilities," Oxford University Press (1932), p. 89.
 19) L. V. Ginzburg, A. A. Gorbatshevich, Yu. V. Kopayev, and B. A. Volkov, *Solid State Commun.* **50**, 339 (1984).